Proceedings of the XVII ECSMGE-2019
Geotechnical Engineering foundation of the future
ISBN 978-9935-9436-1-3

doi: 10.32075/17ECSMGE-2019-0299

Heavy rapid impact compaction for transportation of 13500 ton railway bridge in Muiderberg, the Netherlands

Compactage par impacts rapides pour le transport d'un 13500 tonne pont de voie ferrée à Muiderberg, Pays-Bas.

J. Vink, J.W. Dijkstra
Cofra B.V., Amsterdam, the Netherlands

F.A.J.M Mathijssen
Boskalis/Hydronamic, Papendrecht, the Netherlands

ABSTRACT: The steel structure of a new 265m long railway bridge was moved in place, over one of the major highways in the Netherlands, using two SMPT-groups and temporary structural reinforcement with a total design load of almost 13,500 ton. The bridge was constructed on temporary supports next to the highway. Due to the very high induced loads through the SPMT-groups on the road and the low tolerances in differential settlement during transportation and placement, a stable carriageway needed to be constructed from the construction site up to the placement location. The geological characterisation of the subsoil showed the presence of loose to moderately loose Holocene sand layers with intermediate 1-2m thick peat layers adjacent to and partially present underneath the highway. The theoretical analysis and simulation of transportation of the bridge revealed a large probability of occurrence of large instabilities in the locations with the peat layers and occurrence of static liquefaction resulting in either compaction bands or instabilities in the remaining areas. Based on a critical state soil mechanics framework a minimum compaction boundary was formulated, resulting in a strong dilative response on shear loading at the acting normal forces. In a very short operational window, a partial soil replacement and full surface based compaction was performed using a heavy rapid impact compaction technique called CDC and surface rollers. On critical locations a further improved compaction was achieved by installation of vertical drains. The CDC compaction effort was real time monitored with the on-board system and verified with piezocone testing. The resulting quality approached that of a runway, which proved essential during the actual transportation of the railway bridge.

RÉSUMÉ: La structure en acier d'un nouveau pont de voie ferrée d'une longueur de 265m a été mis en place au-dessus d'une des plus importantes autoroutes des Pays-Bas, au moyen de deux remorques modulaires autopropulsées SPMT et d'un renforcement temporaire de la structure, pour une charge calculée de près de 13500 tonnes. Le pont a été construit sur des supports temporaires à côté de l'autoroute. A cause des importants chargements induits par les ouvrages SPMT sur la route, ainsi que les faibles tolérances de tassements résiduels durant le transport et la mise en place, la construction d'une chaussée stable était requise pour aller du site de construction jusqu'à l'emplacement final. La caractérisation géologique du sous-sol indiquait la présence d'horizons sableux de l'Holocène, lâches à moyennement lâches, avec la présence intermittente de tourbe de 1 à 2m d'épaisseur, à proximité et sous certaines portions de l'autoroute. L'analyse théorique et la simulation de transport du pont a révélé une forte probabilité d'apparition de grandes instabilités aux endroits où la tourbe est repérée d'une part, et une forte probabilité de liquéfaction statique d'autre part. Cela résulterait en bandes compactées ou en instabilités dans les zones adjacentes. A partir d'un cadre de travail critique de mécanique des sols, un critère minimum de compaction a été défini conduisant à une forte dilatance horizontale sous l'effet des forces normales en action. Eu égard au planning restreint, un remplacement partiel du sol et son compactage depuis la surface ont été réalisés au moyen d'une combinaison d'une technique de compactage par impacts rapides dénommée CDC, et de rouleaux compresseurs. Aux emplacements critiques, un compactage plus complexe a été réalisé par l'installation de drains verticaux. Le compactage par CDC a été suivi en temps réel par un système embarqué ainsi que par des tests piezocones. La qualité finale est similaire à celle d'une piste, qui s'est avérée essentielle lors du véritable transport du pont de chemin de fer.

Keywords: Rapid Impact Compaction, Ground Improvement, Static Liquefaction, Vertical Drains, SPMT

1 INTRODUCTION

A section of one of the major highways in The Netherlands, the A1 between Amsterdam and Diemen, has been upgraded with additional lanes between 2014 and 2018. Part of the project was the replacement and the span enlargement of a railway bridge over the highway. As the busy railway and highway were required to remain operational during construction, the steel bridge with a total design load of 13500 ton, almost twice the steel weight of the Eifel tower, was assembled on a temporary location adjacent to the motorway A1 near its final location.

After partial completion, the bridge was transported using two 500m^2 groups of Self Propelled Modular Transporters (SPMT's) over a length of 380m to a temporary foundation next to old bridge where the concrete deck and railway infrastructure was added. From this position, the bridge was horizontally jacked to its permanent position to become part of the existing railway track. Figure 1 provides a top view of the construction site, the transport route and final position of the bridge.

This paper provides background information on the geotechnical risk assessment of the transport, the following design of the ground improvement of the carriageway and the observational method adopted to control the main risks during the transport.

2 THEORETICAL ANALYSIS

The theoretical analysis and risk assessment was performed on the basis of the following three steps:

- Determination of subsoil conditions
- Analysis of the effect of the SPMT load on the encountered soil conditions
- Design of ground improvement and compaction requirement

Figure 1 - Overview: A1 highway, planned carriageway (white borders) and temporary bridge location

2.1 Subsoil conditions

On the basis of a CPTu campaign executed over the complete carriageway three distinct profiles were encountered:
• A soil profile with 1 to 2m of peat (part 1, 2 and 4 of figure 1)
• A soil profile with approx. 0.5-1.5m of peat with a partial soil replacement of sand on top (part 7 and 8 of figure 1)
• A soil Profile without any peat but with a loose sand layer (underneath the highway in part 3, 5 and 6 of figure 1).

All individual profiles, and variations thereof using a stochastic analysis following the work by Fenton & Vanmarcke (1998), were analysed. The Soil Behavior Type index, I_c according to Robertson & Wride (1998) and Robertson (2009) was used for the soil characterisation, which was verified with boreholes and index testing.

2.2 Analysis

The very high loads induced by the two SPMT-groups at each side of the steel bridge and the low tolerances in allowable differential deformation during transportation, resulted in stringent requirements for the allowable subsoil behavior. Using the subsoil characterization in the various sections of the transport lane, various simulations of the bridge transportation were executed and a Performance Based Design was made, where the essential mechanisms ensured a safe transport of the steel bridge in Risk Category 3 (RC-3) according to Eurocode 7 (NEN-EN-9997-1, 2015). During this analysis and simulation top risk events were identified with a strong focus on the short operational window of about a few hours due to the limited time of closure of the highway and the limited allowable distortion of the bridge.

On the basis of the outcome the large volume deformation of the peat and loose sand layers under the sudden load increase were identified as a major risk. Occurrence of large deformations would result in slower and/or stagnation of transport as the SPMT‘s would need jacking or settle out of tolerances. The accompanying result with the occurrence of this risk is the large financial consequence due to not meeting the strict closure deadline of the highway, with very high penalty rates per hour. Another potential result would be that twisted deformation of new railway bridge could occur, resulting in plastic deformation of welds. This in turn could result in the railway authority not taking over the bridge from Rijkswaterstaat (Public works department).

The second major risk was the high chance of the occurrence of static liquefaction of loose sand layers, see next section, resulting in large (>1m thick) instant volume displacements under SPMT transport structure. This may result in a twisted deformation, redistribution of loads and subsequent continued liquefaction. The top event in this case would be overturning of the entire railway bridge as a result of the high center of gravity during transport, due to the fact that the concrete deck is only contsructed after transport to reduce the total weight. In any case, the occurrence of static liquefaction had to be prevented at all cause, since the consequences (closed motorway and building a new bridge) were totally unacceptable.

2.3 Solution

A soil replacement was designed for the areas where peat layers were present and, on the bases of a critical state soil mechanics framework, a minimum compaction requirement was formulated for the complete subsoil underneath the carriageway. The proposed level of compaction was related to a strong dilative response of the sand on shear loading at the acting normal forces from the SPMT-groups. The next chapter will provide a further insight into the design of the requirements.

3 GROUND IMPROVEMENT REQUIREMENT

Based on a critical state soil mechanics framework a minimum compaction boundary was formulated.

3.1 Static liquefaction boundary

The factors that control the occurrence of unstable behavior have been investigated by Lade (1989). Materials exhibiting non-associated flow may become unstable when exposed to certain stress paths inside the Mohr-Coulomb failure surface. However, it is emphasized by Lade (1989) that instability is not synonymous with failure, although it may lead to catastrophic events.

In Figure 2 a schematic presentation of the location of the instability line for loose sand is presented in (p`,q) plane, with p` being the isotropic effective stress and q the deviatoric stress while applying soil mechanics' sign convention (compression positive). The top of the yield surface of the non-associatively flowing loose sand lies within the failure surface, while after large straining and development of softening, the failure surface is reached.

Following the work of Roscoe et al. (1958), the softening frictional fluid flow will eventually reach the critical state line (CSL) as failure surface, but the state (p`, e, q) at which the CSL is reached is significantly different from its initial unstable state. The line from the origin in p`, q space to the top of the yield surface is defined as the instability line. The slope of this instability line, M_{IL} is not constant and depends for a certain material on the initial void ratio at the instability point, e (Figure 2).

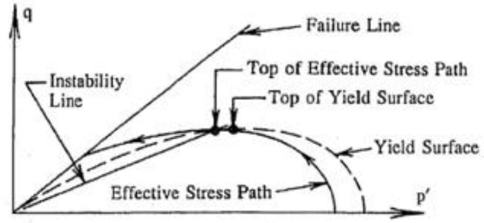

Figure 2 - Location instability line for loose sand (Fig. 7 – Lade, 1992)

Been & Jefferies (1985) proposed a state parameter for sand which defines the distance in void ratio from the corresponding point on the CSL in void ratio – stress space. Contrary to the relative density, the state parameter has proven to describe a contractive behavior for a positive state parameter and dilative behavior for a negative state parameter, for the whole engineering stress range. According to Jefferies & Been (2006), the transition in behavior lies around a modified state parameter $\bar{\psi} = -0.07$, due to the fact that in triaxial compression even samples starting at the critical state show an initial tendency for softening followed by a dilatant response.

The state parameter approach fits therefore well in the Critical State framework. The in-situ characterisation and determination of the state parameter using piezocone testing (CPTu) is very cost effective, yet associated with quite some uncertainty.

The CPTu data and some density cone data were converted into relative density and state parameter profiles by using correlations from Lunne et al. (1997) and Shuttle et al. (1998).

The amount of uncertainty involved in the direct or indirect state parameter determination was significant ($\bar{\psi} \pm 0.05$) where the indirect, relative density based, method resulted in a lower boundary ($\bar{\psi} -0.10$), which was adopted for project application

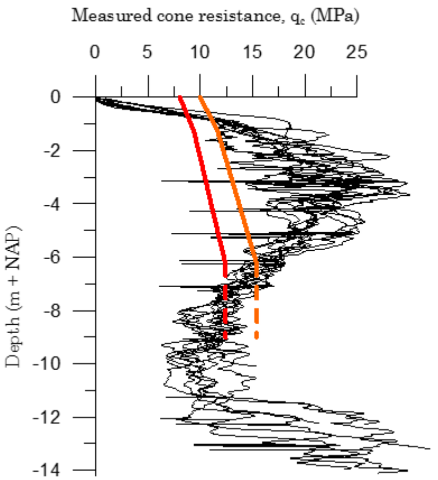

Figure 3 – Minimum (red) and target (orange) compaction requirements with CPT results in one section versus depth.

In Figure 3, the minimum compaction requirement, corresponding to $\overline{\psi}$ -0.07, and the target compaction requirement, corresponding to $\overline{\psi}$ -0.10, are presented together with the CPTu results after compaction in one area. The target compaction requirement proposed by Robertson (2010) corresponds to a normalized cone resistance Q_{tn} of 73.

The limiting depth is determined by the (q/p`)-ratio imposed by the moving SPMT loads over the surface, estimated using elasticity theory according to Timoshenko & Goodier (1951), and the estimated resulting instant compaction, making reference to the work by Ishihara & Yoshimine (1992).

3.2 FEM simulations

Finite Element Model simulations were performed, for the subsoil with the envisaged compaction quality of the sand layer overlying the moderately compacted underlying sand layer.

The well validated (Schanz et al, 1999) Hardening Soil model proposed by Vermeer (1978) was used to model the sand behavior. It should be noted that in this particular model an isotropic hardening rule is assumed, where Koiter (1953) has pointed out that for anisotropic material behavior a significant lower yield strength may be encountered depending on loading conditions and state.

The main purpose of the FEM simulations was therefore firstly to determine the maximum principal stress gradient in the subsoil stratum assuming drained soil behavior and secondly to perform undrained stress path simulations to predict the generated excess pore water pressure response. With the observational method (Peck, 1969) in mind, the results of the simulations were used to determine the location and accuracy of the piezometers, which were installed to monitor the actual transportation process.

4 COMPACTION OPERATIONS

After the soil replacement, a very short operational window was available for the compaction of the complete surface of the carriageway using a heavy 16 tons Rapid Impact Compaction technique (RIC) called Cofra Dynamic Compaction (CDC). Figure 5 shows the system in which a 16 ton weight is repeatedly dropped from a predetermined height onto a foot which remains, during the compaction, in contact with the subsoil. The foot diameter is chosen such that it is not driven down into the soil like a pile, but vibrations are generated that in turn densify the granular soil. The compaction process of a location is continued until the maximum stroke of the hammer or another stop criteria is met. The zone of influence in depth has a spherical shape and reaches up to 9m, depending on subsoil conditions.

Figure 4 – Compaction operations next to the tem-porary bridge location

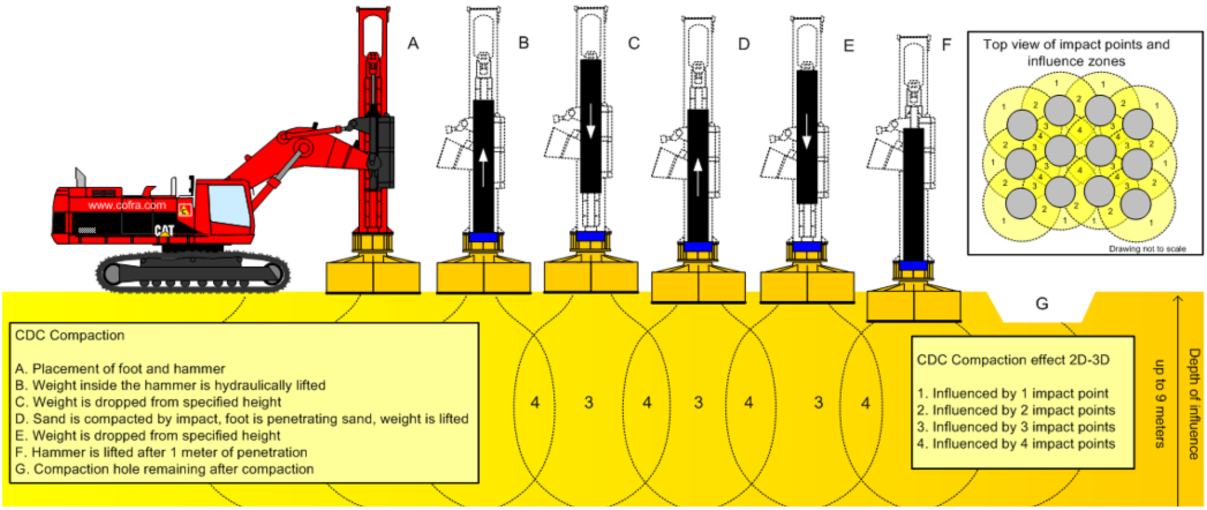

Figure 5 – CDC Compaction work method and compaction influence

4.1 Suitability of the technique

The method was chosen as most suitable for this project because of the following reasons:

- The depth of influence coincided with the requirements
- Homogeneous compaction, with overlapping influence zones was required
- Very high compaction levels were required to be achieved in the top 6.5m, see figure 3
- High production rates were required due to the available time for the compaction of the highway stretches in weekend closures
- A safe method with no free falling objects was required due to work within 2 meter of a main highway
- A good quality control system needed to be in place to monitor the compaction.

4.2 Quality control

The onboard Crane Monitoring System (CMS) logs the different parameters amongst the total settlement, number of blows and the settlement per blow which is correlated to the end resistance of the subsoil. This was used to identify soft spots and monitor the compaction levels over the causeway.

Figure 6 gives an example of the total settlement of compaction points and shows the loose (high settlement) highway stretches. Red represents high settlements and green relatively low settlements. From the data it can be observed that compaction on a part of the A1 generated a settlement of almost 1m.

After finishing the compaction works the logger data was combined with interpreted CPTu results and plotted in this overview. This was used for a monitoring plan and during transportation of the Bridge which is discussed in the next section.

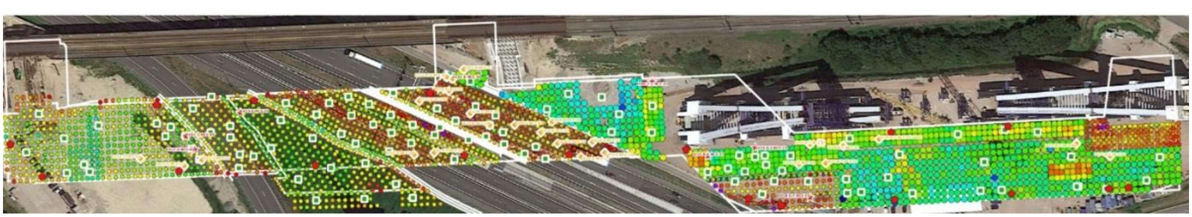

Figure 6 – CDC Logger data results on carriageway including CPTu locations

4.3 Operational challenges

4.3.1 (no) time

The Main challenge of the project was the (no) time. On some sections, 3, 4, 5 and 6 of figure 1, time slots of 8 to 12 hours were available to compact and test the soil before the base layer and asphalt needed to be placed to have traffic flowing in time. Two rigs were mobilized to assure continuation in the unlikely event one of the machines broke down.

4.3.2 Pore pressures

Compaction often took place just after the soil replacement, in which very loose sand was placed under the water level with a high void ratio and water content. Due to the limited extent of the soil replacements and the fast compaction (a location takes less than a minute to compact) large strains were induced. This led to high pore pressures and at a few locations loss in strength. Under normal conditions a lower compaction energy would be applied over multiple compaction passes, gradually increasing the compaction energy and leaving enough time in between the compaction passes. In this project this was not possible and Prefabricated Vertical Drains (PVD's) were used to dissipate the excess water.

They proved to work very well, this can be observed in figure 7 which shows a drain that is discharging water at a high rate due to nearby compaction. The drains continued with the high discharge rate hours after compaction was performed.

Figure 7 – Vertical drains discharging compaction induced excess pore water

4.3.3 CPT Results

The compaction induced excess pore pressures in the sand influenced CPT cone tip resistance results in case the CPT was performed shortly after compaction, predominantly in areas where a very recent soil replacement was performed. Especially in the top layer the requirements were sometimes not directly reached even after 2 or 3 compaction passes (even with the PVD's in place). An example is given on figure 8 (left) which illustrates the CPT results just after the first (AC1), the second (AC2) and even a third pass (AC3) with CDC – represented by the red, the green and the black line respectively. As can be observed from the graph there is little to no improvement in the top 4m. During these CPT tests the water was still flowing up through the surface and vertical drains, clearly indicating excess pore water pressures. The graph also shows a test nearby that was performed after another compaction pass and a resting period of approx. 2 days, clearly showing an increase in of 5-10Mpa in the top layer which is caused by the dissipation of water pressures.

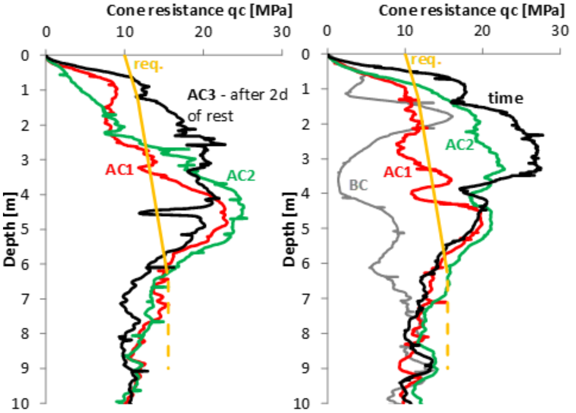

Figure 8 – Left: CPT results just after soil replacement and compaction and after a period of rest, right: typical average cone resistance before and after compaction (2nd pass) in Area 1/2

Figure 8 (right) shows an example of a typical CPT with the average CPT cone resistance before (BC) and after compaction (AC1 & AC2) in area

1/2 (figure 1). As can be observed the influence depth of compaction, i.e. the depth where a cone resistance increase visible, is around 7.5-8m with a significant increase of cone resistance in the top 6m. There is also clearly a significant increase of cone resistance in the top 4m of the CPT‘s taken after a rest period of approx. 30d. Over this relatively short time span it is expected to be caused mainly by the further dissipation of excess pore water pressures and possibly some slight aging effects (chemical bonding).

5 MEASUREMENTS DURING TRANSPORTATION / OBSERVATIONAL METHOD

Prior to the actual transport operation a detailed risk analysis was performed and all main mechanisms and resulting risks were controlled following the observational method by Peck (1969).

The following four main mechanisms were identified, monitored and controlled from one main control room on site:

* Wind speed ≥ 15m/s would overload the allowable pressure of the hydraulic system, necessitating the halting of the transport operation. A real-time local weather forecast system was in place to predict a safe operational window and ensure a safe working platform.

* Partial liquefaction/compaction of deeper sand layer due to undrained response resulting in a non-uniform load and/or local instabilities. Both the hydraulic pressures of the front and aft system and excess pore water pressure underneath the runway in that layer were realtime monitored allowing for the control of the transportation speed.

* Occurrence of a differential deformation of the carriage-system and pavement larger than allowed by the SPMT system, crossing the existing road alignment, was real-time monitored with a closed grid of scanning total stations and mounted reflectors on the SPMT-groups. In case of a developing excessive deformation, the two SPMT-groups would drive back at a safe distance and emergency pavement would be placed.

* Twisted deformation of the two bridge arches could result in the plastic deformation of welds. This risk was mitigated by real-time leveling of the individual SPMT groups with inclinometers and lasers. One live image on a handheld allowed the SPMT operator at the bridge to control the whole transport operation.

The extensive preparations and use of one central control room and live link to the operator paid off during the whole operation. The CDC compacted runway showed a dilatant behavior, which allowed for a 3 hour faster bridge transport than its earliest anticipated arrival.

Figure 9 – Bridge just before transportation

6 CONCLUSION

Soil replacement and compaction on the causeway for the Railway bridge has been successfully performed, which mitigated the most predominant risks.

The remaining possible failure mechanisms could be controlled with the observational method by means of the extensive monitoring program and live control room with direct link to the central SPMT-operator. Numerous simulations were performed and scenarios ready for direct operation if needed to ensure a smooth and safe transport of this exceptional load of the main highway in the Netherlands.

The system behavior, comprising of CDC compacted subsoil, pavement and SPMT-groups, behaved superbly resulting in marginal deformations on the road and relative under pressures in the piezometers indicating a dilative soil behavior.

The relative deformation measurements of the two arches of the bridge stayed in the predefined green area, proving unaffected high-quality of the bridge due to transportation over this well-compacted runway.

7 ACKNOWLEDGEMENTS

We would like to thank all partners in the contractors combination SAAone for the close cooperation in this multi-disciplinary project, which was the key to its success.

8 REFERENCES

Been, K. & Jefferies, M.G. (1985) A state parameter for sands, *Géotechnique* **35**(2), 99-112.

Cai, Y., Sun, H., & Xu, C. (2007) Steady state response of poroelastic half-space soil medium to a moving rectangular load. *Int. J. Solids & Structures* 44, 7183-7196.

Fenton, G.A., & Vanmarcke, E.H. (1998) Spatial variation in liquefaction risk. *Géotechnique* **48**(6), 819–831.

Ishihara, K. (1985) Stability of natural deposits during earthquakes. *Proc. 11th Int. Conf. on Soil Mechanics and Foundation Engineering*, San Francisco 2: 321-376.

Ishihara, K., & Yoshimine, M. (1992) Evaluation of settlements in sand deposits following liquefaction during earthquakes. *Soils and Foundations* **32**(1), 173-188.

Jefferies, M.G. & Been, K. (2006) Soil liquefaction. A critical state approach, *Taylor & Francis*, Oxon (UK).

Koiter, W. T. (1953) Stress-strain relations, uniqueness and variational theorems for

elastic-plastic materials with a singular yield surface. *Q. appl. Math.* **11**, 350-354

Lade, P.V. (1989) Instability and failure of soils with nonassociative flow. *Proc. 12th ICSMFE. Rio de Janeiro, Brazil* **1**: 727-730.

Lade, P.V. (1992) Static instability and liquefaction of loose fine sandy slopes. *Journal of Geotechnical Engineering* **118**(1), 51-71.

Mathijssen, F.A.J.M., de Jager, R.R., & Hooiveld, B.J. (2015) Reliability based design of dredge sludge depot for mechanism static liquefaction. *Geotechnical Safety and Risk V, ISGSR 2015.* Rotterdam, the Netherlands. IOS Press: 320-327.

NEN-EN 9997-1 + C2 (2016) Eurocode 7: Geotechnical Design of structures – Part 1: General rules, NNI, Delft.Peck, R. B. (1969) Advantages and Limitations of the Observational Method in Applied Soil Mechanics. *Géotechnique* **19**(2), 171–187.

Robertson, P. K. (2009) Interpretation of cone penetration tests - a unified approach. *Can. Geotech. J.* **46**(11), 1337-1355.

Robertson, P.K. (2010) Evaluation of Flow Liquefaction and Liquefied Strength Using the Cone Penetration Test. *Journal of geotechnical and geoenvironmental engineering* **136**(6), 842-853.

Robertson, P. K., & Wride, C.E. (1998) Evaluating cyclic liquefaction potential using the cone penetration test. *Can. Geotech. J.* **35**(3), 442-459.

Roscoe, K. H., Schofield, A. N., & Wroth, C.P. (1958) On The Yielding of Soils. *Géotechnique* **8**(1), 22–53.

Schanz, T., Vermeer, P.A., & Bonnier, P.G. (1999) Hardening soil model: Formulation and verification. *Beyond 2000 in computational geomechanics - 10 years of Plaxis.* A.A. Balkema: 1-16.

Timoshenko, S.P. & Goodier, J.N. (1951) Theory of elasticity, McGraw-Hill book company, inc.

Vermeer, P.A. (1978) A double hardening model for sand. *Géotechnique* **28**(4), 413–433.